© 2017. Published by The Company of Biologists Ltd | Development (2017) 144, 235-247 doi:10.1242/dev.138099

Ascl2 inhibits myogenesis by antagonizing the transcriptional activity of myogenic regulatory factors

Chao Wang[1], Min Wang[1], Justine Arrington[2], Tizhong Shan[1], Feng Yue[1], Yaohui Nie[1], Weiguo Andy Tao[3,4] and Shihuan Kuang[1,4,*]

ABSTRACT

Myogenic regulatory factors (MRFs), including Myf5, MyoD (Myod1) and Myog, are muscle-specific transcription factors that orchestrate myogenesis. Although MRFs are essential for myogenic commitment and differentiation, timely repression of their activity is necessary for the self-renewal and maintenance of muscle stem cells (satellite cells). Here, we define Ascl2 as a novel inhibitor of MRFs. During mouse development, Ascl2 is transiently detected in a subpopulation of Pax7$^+$ MyoD$^+$ progenitors (myoblasts) that become Pax7$^+$ MyoD$^-$ satellite cells prior to birth, but is not detectable in postnatal satellite cells. *Ascl2* knockout in embryonic myoblasts decreases both the number of Pax7$^+$ cells and the proportion of Pax7$^+$ MyoD$^-$ cells. Conversely, overexpression of *Ascl2* inhibits the proliferation and differentiation of cultured myoblasts and impairs the regeneration of injured muscles. Ascl2 competes with MRFs for binding to E-boxes in the promoters of muscle genes, without activating gene transcription. Ascl2 also forms heterodimers with classical E-proteins to sequester their transcriptional activity on MRF genes. Accordingly, MyoD or Myog expression rescues myogenic differentiation despite Ascl2 overexpression. *Ascl2* expression is regulated by Notch signaling, a key governor of satellite cell self-renewal. These data demonstrate that Ascl2 inhibits myogenic differentiation by targeting MRFs and facilitates the generation of postnatal satellite cells.

KEY WORDS: Ascl2, MRF, Repressor, Myogenic progenitor cell, Self-renewal

INTRODUCTION

Development of skeletal muscle is a highly orchestrated process regulated by several basic helix-loop-helix (bHLH) proteins known as myogenic regulatory factors (MRFs) (Olson and Klein, 1994; Pownall et al., 2002), including Myf5, MyoD (Myod1), Myog and Myf6 (Mrf4). Each MRF alone can transform non-myogenic fibroblastic cells into myoblasts (Braun et al., 1989; Davis et al., 1987; Edmondson and Olson, 1989; Rhodes and Konieczny, 1989). Myf5, MyoD and Myf6 play redundant roles in committing somite-derived cells to myoblasts (Kassar-Duchossoy et al., 2004; Rudnicki et al., 1993). MyoD and Myf6 also initiate the onset of myogenic differentiation (Rawls et al., 1998). In turn, Myog governs myoblast terminal differentiation (Hasty et al., 1993). MRFs typically form heterodimers with ubiquitous bHLH proteins, also known as E-proteins, consisting of TCF4 (E2-2), TCF12 (HEB) and TCF3 (E2A, E47). The heterodimers subsequently bind to a hexameric consensus DNA sequence, the E-box (CANNTG), to activate the transcription of target genes (Lassar et al., 1991; Zhang et al., 1999).

Satellite cells are muscle stem cells that reside between the sarcolemma and basement membrane of myofibers (Mauro, 1961), and are responsible for postnatal muscle growth and regeneration (Kuang and Rudnicki, 2008). Satellite cells are derived from a primitive myogenic progenitor population that expresses the paired box transcription factors Pax3 and Pax7 in the dermomyotome (Kassar-Duchossoy et al., 2005; Relaix et al., 2005). Pax3 is downregulated, but Pax7 is maintained, during fetal myogenesis (Kassar-Duchossoy et al., 2005). At the end of the fetal stage, Pax7$^+$ cells locate beneath the basal lamina and outside the fiber, a characteristic of satellite cells (Kassar-Duchossoy et al., 2005). Once the muscle has matured, these Pax7$^+$ cells enter a quiescent state as satellite cells (Bentzinger et al., 2012). Whereas lineage-tracing results show that most satellite cells have expressed Myf5, Myf6 and MyoD during development (Günther et al., 2013; Kanisicak et al., 2009; Kuang et al., 2007; Sambasivan et al., 2013), MyoD and Myf6 are rarely detectable in quiescent satellite cells (Kanisicak et al., 2009; Zammit et al., 2002). It is therefore hypothesized that a portion of Pax3/7$^+$ MyoD$^+$ cells revert to Pax7$^+$ MyoD$^-$ cells to become satellite cells during fetal myogenesis. This process involves upregulation of Pax7 and downregulation of MyoD. In addition to the control of MyoD expression, the transcriptional activity of MyoD itself is also repressed by various factors. For example, MyoR (Msc), a bHLH factor that inhibits the activity of MyoD through competitively sequestering E-proteins and binding with the E-box, is involved in the maintenance of myogenic progenitor cells (Lu et al., 1999).

Ascl2 (Mash2, Hash2) is a bHLH transcription factor homologous to a protein of the Achaete-Scute complex in *Drosophila* (Johnson et al., 1990). Its expression is predominantly detected in extraembryonic tissues, where it controls placenta development (Guillemot et al., 1994). In adult tissues, Ascl2 is mainly found in the intestine, where it plays an indispensable role in the maintenance of intestinal stem cells (van der Flier et al., 2009). Other studies indicate that Ascl2 is also expressed in skin epidermis and Schwann cells (Kury et al., 2002; Moriyama et al., 2008). A recent study reports that Ascl2 initiates the development of T-helper cells (Liu et al., 2014). In the present study, we report a novel role of Ascl2 in facilitating the generation of muscle satellite cells through inhibiting MRFs in embryonic myoblasts.

RESULTS

Ascl2 expression in myogenic cells

First, we examined Ascl2 protein levels in hindlimb muscles of mice at different developmental stages, including embryonic (E) day 17.5

[1]Department of Animal Science, Purdue University, West Lafayette, IN 47906, USA. [2]Department of Chemistry, Purdue University, West Lafayette, IN 47906, USA. [3]Department of Biochemistry, Purdue University, West Lafayette, IN 47906, USA. [4]Center for Cancer Research, Purdue University, West Lafayette, IN 47906, USA.

*Author for correspondence (skuang@purdue.edu)

S.K., 0000-0001-9180-3180

Received 31 March 2016; Accepted 6 December 2016

Development (2017) 144, 235-247 doi:10.1242/dev.138099

and postnatal (P) day 1, 14 and 60 (Fig. 1A). The specificity of the Ascl2 antibody is validated by a positive control using cell lysates of primary myoblasts transduced with an *Ascl2-FLAG* adenoviral vector (Fig. 1A). This analysis indicates that the protein levels of Ascl2 are higher at E17.5 and P1, but dramatically lower at P14 and undetectable at P60 (Fig. 1A). Interestingly, a weak, larger band was detectable in the muscles (Fig. 1A), suggesting a potential post-translational modification of Ascl2. Consistently, the mRNA levels of *Ascl2* also declined gradually from E17.5 to P60 (Fig. 1B).

We further performed immunohistochemical staining on cross-sections of embryonic myotomes and postnatal tibialis anterior (TA) muscles using the Ascl2 antibody as validated by staining C2C12 cells transduced with *Ascl2-GFP* adenoviral vectors (Fig. S1A). At E10.5, when primary myogenesis begins, Ascl2 expression is undetectable in the myotomes (Fig. S1B). At E12.5, when primary myogenesis peaks, Ascl2 is expressed in a small subset (~3%) of $Pax7^+$ cells, and most (~80%) of these $Ascl2^+$ cells also expressed MyoD (Fig. 1C, Fig. S1B). These results indicate that Ascl2 is primarily expressed in $Pax7^+$ $MyoD^+$ cells. At E17.5, when secondary myogenesis peaks, ~3% of $Pax7^+$ cells expressed Ascl2 in the back muscle (Fig. 1D, Fig. S1B,C). These $Pax7^+$ $Ascl2^+$ cells are located beneath the basal lamina, where quiescent satellite cells are found (Fig. S1C). By contrast, none of the $MyoD^+$ cells expressed Ascl2 (Fig. 1D, Fig. S1D), indicating that Ascl2 is only expressed in $Pax7^+$ $MyoD^-$ cells that are primed to become satellite cells (Kassar-Duchossoy et al., 2005; Relaix et al., 2005). At P1, we observed Ascl2 expression in the nucleus of ~1% of $Pax7^+$ cells in TA muscles (Fig. S1B,E). However, Ascl2-positive signals were undetectable in TA muscles of adult mice (Fig. S1B). The sequential reduction of Ascl2 immunofluorescence from embryonic to postnatal myogenesis mirrors the protein and mRNA expression patterns that we had determined.

Loss of Ascl2 inhibits the generation of $Pax7^+$ cells during embryogenesis

To investigate the role of Ascl2 in embryonic myoblasts, we generated a myoblast-specific *Ascl2* knockout mouse model: $Pax3^{Cre/+}/Ascl2^{flox/flox}$ (KO) mice. We examined Ascl2 protein levels in hindlimb muscles of E17.5 $Pax3^{+/+}$ (WT) and KO mice. As expected, Ascl2 bands were detectable in WT but not in KO muscles

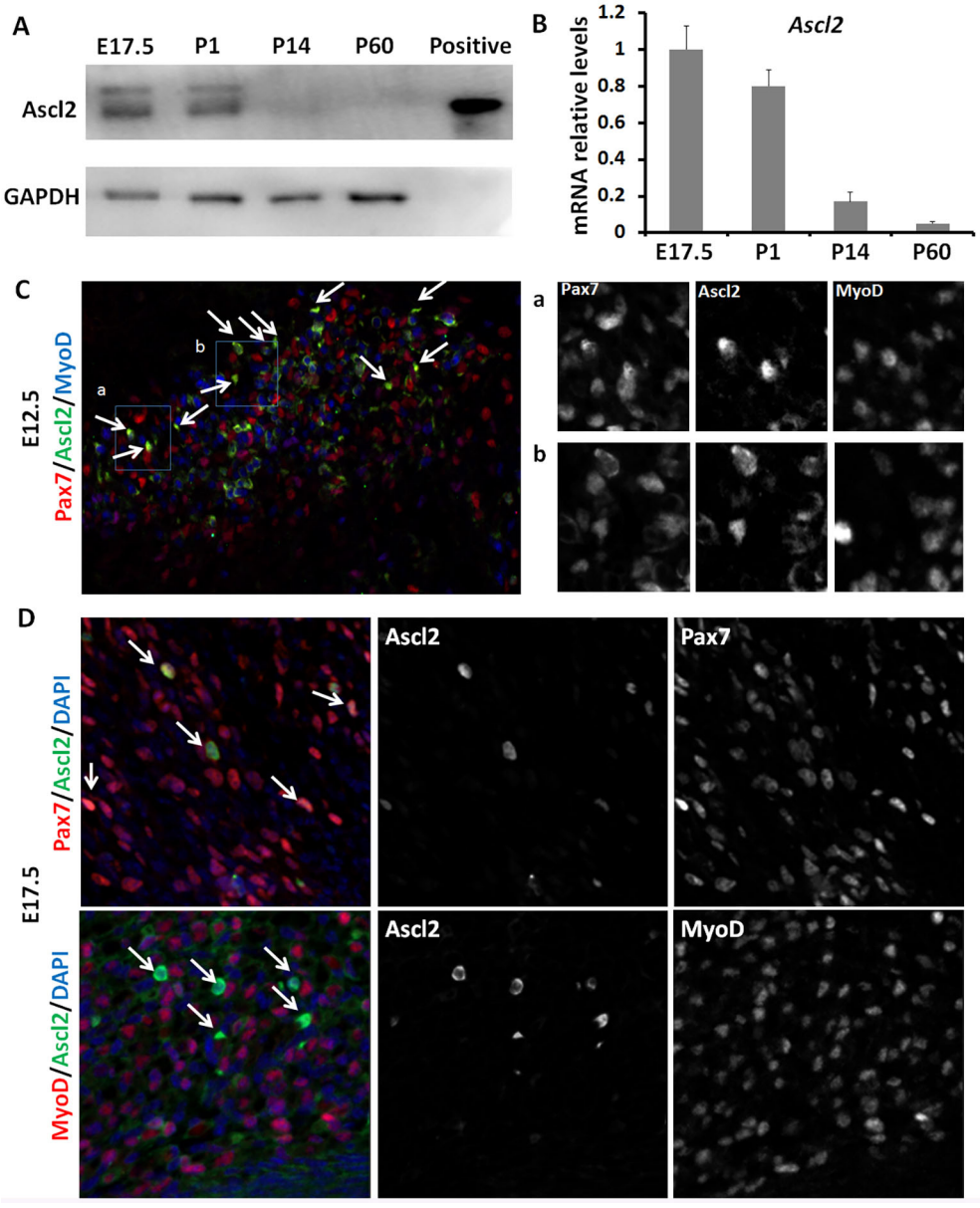

Fig. 1. Expression of Ascl2 in mouse muscle tissues. (A,B) Expression levels of Ascl2 in hindlimb muscles at different developmental stages (E17.5, P1, P14 and P60) as determined by western blot (A) and qPCR (B). At E17.5 and P1 the whole hindlimb muscles were sampled; at P14 and P60 the TA muscles were sampled. Error bars represent mean and s.d. of four mice. The positive control in A is cell lysates of primary myoblasts transduced with an Ascl2-FLAG adenoviral vector. (C) Immunostaining of Ascl2 (green), Pax7 (red) and MyoD (blue) in epaxial myotome regions at E12.5. Arrows indicate $Ascl2^+$ cells. Representative regions (a,b) are shown at higher magnification. (D) Immunostaining of Ascl2 (green), Pax7 (red), MyoD (red) and DAPI staining (blue) in back muscles at E17.5. Arrows indicate $Ascl2^+$ cells.

Development (2017) 144, 235-247 doi:10.1242/dev.138099

(Fig. 2A). Body weights of E17.5 WT and *Pax3*$^{Cre/+}$/*Ascl2*$^{flox/+}$ (HE) mice were comparable and 20% heavier than that of KO mice (Fig. 2B). To exclude the possibility that phenotypes are due to the expression of Cre recombinase or Pax3 deficiency, we compared muscles from E17.5 HE and KO mice. Consistently, Ascl2 was detectable in Pax7^{+} cells of HE but not KO mice (Fig. 2C). Total numbers of myofibers in TA muscles were identical in HE and KO mice (Fig. 2D), but there were significantly fewer Pax7^{+} cells in KO than in HE mice (Fig. 2E,F). Notably, clusters of small myofibers appeared among normal myofibers in the KO but not HE mice (Fig. 2E), leading to a smaller average myofiber diameter in KO mice (Fig. 2G). We further labeled myoblasts with Pax7 and MyoD antibodies and found that the proportion of 'reserved' cells (Pax7^{+} MyoD^{-}) was significantly lower in KO than in HE mice (Fig. 2H,I), suggesting that *Ascl2* knockout promoted Pax7^{+} cells to express MyoD. These results indicate that Ascl2 suppresses MyoD expression in embryonic myoblasts.

We further examined the regenerative response of acutely injured TA muscles of 2-month-old WT and KO mice. The regenerative efficiency was evaluated at 7 and 21 days post injury (dpi) (Fig. S2A). The muscle regeneration of KO mice was normal (Fig. S2A), and the size of regenerated myofibers of KO mice was comparable to that of WT mice at both time points (Fig. S2B). We conclude that Ascl2 specifically functions during embryonic myogenesis.

Ascl2 inhibits the proliferation of myoblasts

To understand the role of Ascl2 in myogenesis, we examined the proliferation of Ascl2-expressing cells using Ki67 as a marker. At both E12.5 and E17.5 Ascl2^{+} cells were predominantly Ki67^{-} (Fig. 3A), suggesting that Ascl2^{+} cells were not proliferative *in vivo*. To confirm the role of Ascl2 in proliferation, we used adenovirus to overexpress *Ascl2-GFP* (Ascl2^{OE}) or *GFP* only (as control) in adult primary myoblasts. One day after incubation with adenovirus in growth medium, ~55% of myoblasts had GFP signals in both Ascl2^{OE} and control groups (Fig. 3B), indicative of similar infection efficiencies. The cells were then allowed to grow in virus-free medium for 5 more days, during which time the proportion of GFP^{+} cells was reduced to 40% in the control group but to 9% in the Ascl2^{OE} group (Fig. 3C), indicating that Ascl2 inhibits cell

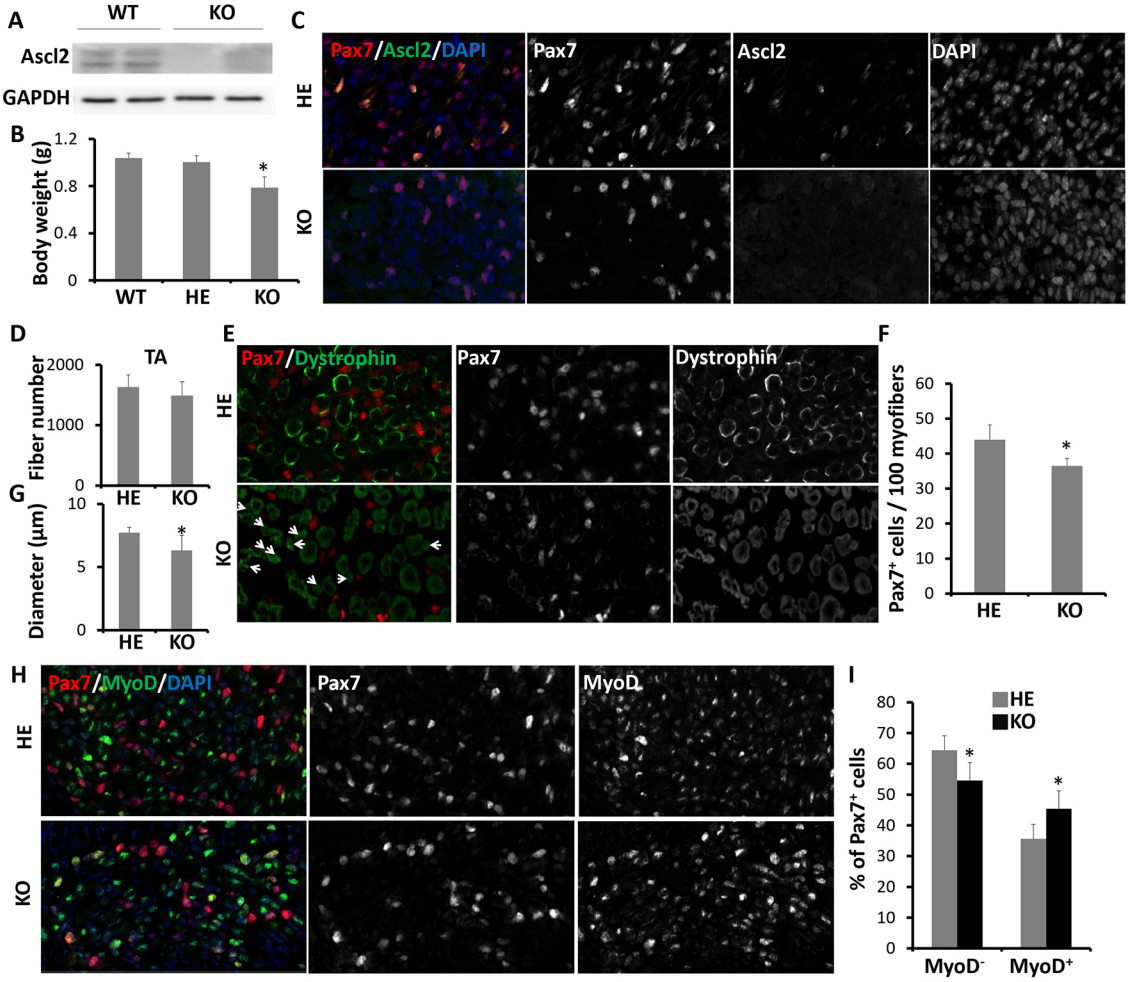

Fig. 2. Loss of Ascl2 in embryonic myoblasts influences the generation of Pax7^{+} cells. (A) The expression levels of Ascl2 in hindlimb muscles of *Pax3*$^{+/+}$ (WT) and *Pax3*$^{Cre/+}$/*Ascl2*$^{flox/flox}$ (KO) E17.5 mice as determined by western blot. (B) Body weights of WT, *Pax3*$^{Cre/+}$/*Ascl2*$^{flox/+}$ (HE) and KO E17.5 mice. Error bars represent mean with s.d. of 6, 4 and 4 mice for WT, HE and KO, respectively. (C) Immunostaining of Pax7 (red), Ascl2 (green) and DAPI staining (blue) in back muscles of HE and KO mice at E17.5. (D) Fiber numbers of TA muscles in the distal limbs of HE and KO mice at E17.5. (E) Immunostaining of Pax7 (red) and dystrophin (green) in back muscles of HE and KO mice at E17.5. Arrows highlight small myofibers. (F,G) Quantification of the number of Pax7^{+} cells per 100 myofibers outlined by dystrophin (F) and the diameter of myofibers (G) based on the images in E. (H) Immunostaining of Pax7 (red), MyoD (green) and DAPI staining (blue) in back muscles of HE and KO mice at E17.5. (I) Quantification of the percentage of MyoD^{-} or MyoD^{+} cells among Pax7^{+} cells. Two different areas were analyzed for each section, and six sections were analyzed for each sample. Error bars represent mean with +s.d. of four mice. *P<0.05 (Student's t-test).

Development (2017) 144, 235-247 doi:10.1242/dev.138099

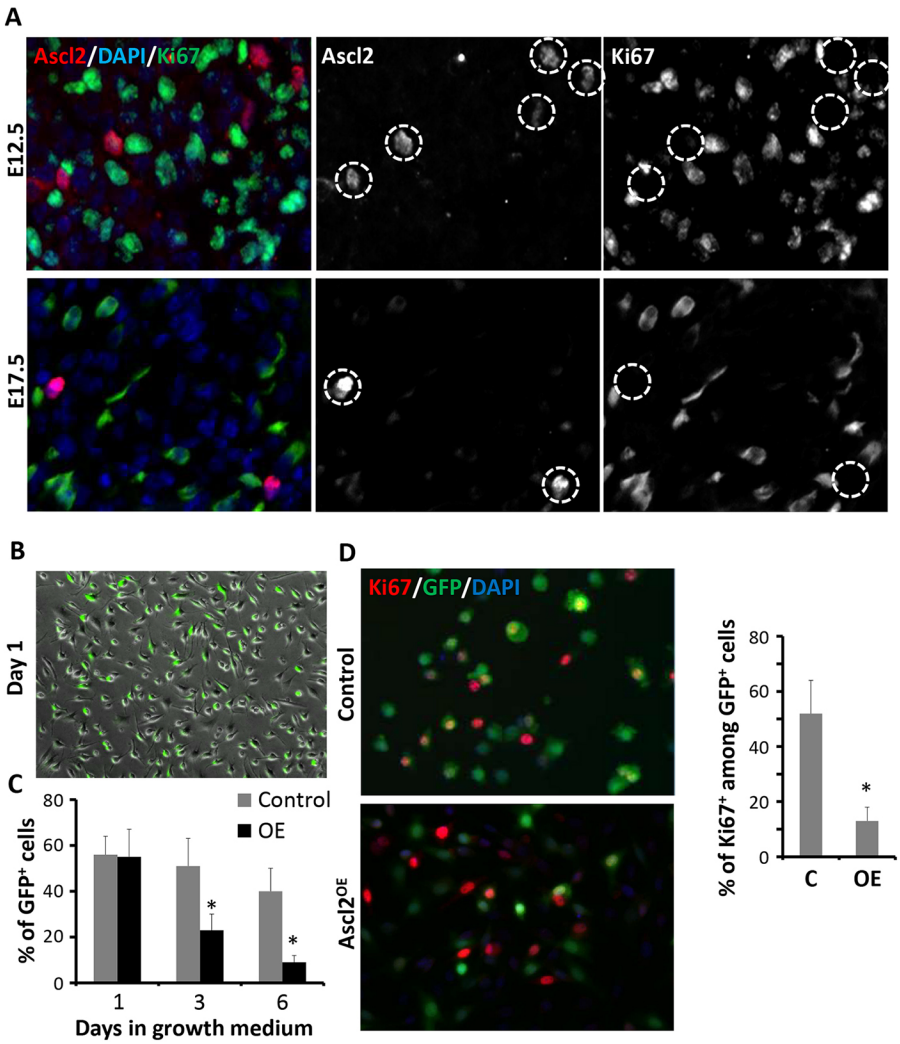

Fig. 3. Ascl2 inhibits myoblast proliferation. (A) Immunostaining of Ascl2 (red), Ki67 (green) and DAPI staining (blue) in epaxial myotome and back muscle regions at E12.5 and E17.5, respectively. Ascl2^{+} cells were negative for Ki67 (circled). (B) A representative field showing infection efficiency (indicated by GFP expression) at day 1 after transduction with adenovirus expressing GFP or Ascl2-GFP. (C) The ratio of GFP^{+} cells at different time points after adenovirus infection for GFP control or Ascl2-GFP. (D) Ki67 expression (red) among Ascl2^{OE} or control cells (GFP^{+}). Five different areas were analyzed in each experiment. Error bars represent mean with s.d. of three independent biological replicates. *P<0.05 (Student's t-test).

proliferation or induces cell death. To distinguish these possibilities, we colabeled the cells with Ki67. Whereas 52% of GFP^{+} cells were also Ki67^{+} in the control group, only 13% of the GFP^{+} cells were Ki67^{+} in the Ascl2^{OE} group (Fig. 3D). These results provide direct evidence that Ascl2 inhibits myoblast proliferation.

Ascl2 inhibits the differentiation and fusion of primary myoblasts

To further investigate the role of Ascl2 in myogenesis, we compared the differentiation of Ascl2^{OE} and control myoblasts. Within 1 day of serum withdrawal-induced differentiation, control myoblasts already displayed an obviously elongated morphology, a hallmark of differentiation (Fig. 4A). By contrast, Ascl2^{OE} myoblasts were mostly still spherical (Fig. 4B), indicative of a differentiation defect. We quantified the differentiation index, which measures the fraction of myonuclei that are located in myosin heavy chain-expressing (MF20^{+}) cells. Whereas 80% of nuclei in the control group were located in MF20^{+} cells, only 23% of nuclei in the Ascl2^{OE} group were located in MF20^{+} cells (Fig. 4C). Therefore, overexpression of Ascl2 in proliferating myoblasts inhibits their subsequent differentiation.

To overcome the confounding effect of Ascl2 on myoblast proliferation, we also used adenovirus to overexpress *Ascl2* or *GFP* in differentiating myoblasts 1 day after serum withdrawal. After differentiation for an additional 2 days, both GFP-expressing and Ascl2^{OE} myoblasts displayed elongated morphology and were MF20^{+} (Fig. 4D,E). However, whereas the control myoblasts formed uniformly aligned multinucleated myotubes (Fig. 4D), most Ascl2^{OE} myoblasts contained only one nucleus (Fig. 4E), indicative of a fusion defect. We quantified the fusion index, which measures the percentage of myonuclei present in multinucleated myotubes. About 63% of control myonuclei were located within multinucleated myotubes, whereas only 9% of Ascl2^{OE} myonuclei formed myotubes containing two or more nuclei (Fig. 4F). We conclude that overexpression of Ascl2 inhibits the differentiation and fusion of primary myoblasts.

Ascl2 overexpression impairs muscle regeneration *in vivo*

We further investigated how Ascl2 affects skeletal muscle regeneration *in vivo* after adenovirus-mediated overexpression of Ascl2-GFP or GFP (control). TA muscles were bilaterally injured with CTX and the left and right TA muscles were injected with Ascl2^{OE} or control adenovirus, respectively, at 2 dpi. At 7 dpi, both Ascl2^{OE} and control adenovirus-injected TA muscles exhibited strong GFP signals throughout the entire TA muscle section (Fig. 5A), indicating high efficiency of adenoviral infection. As expected, TA muscles injected with Ascl2^{OE} adenoviruses exhibited substantial (>1700-fold) increases in *Ascl2* mRNA levels (Fig. 5B). Ascl2 protein was also detected in Ascl2^{OE} TA muscles (Fig. S3A). Ascl2^{OE} did not affect the weight of TA muscles, but impaired

Development (2017) 144, 235-247 doi:10.1242/dev.138099

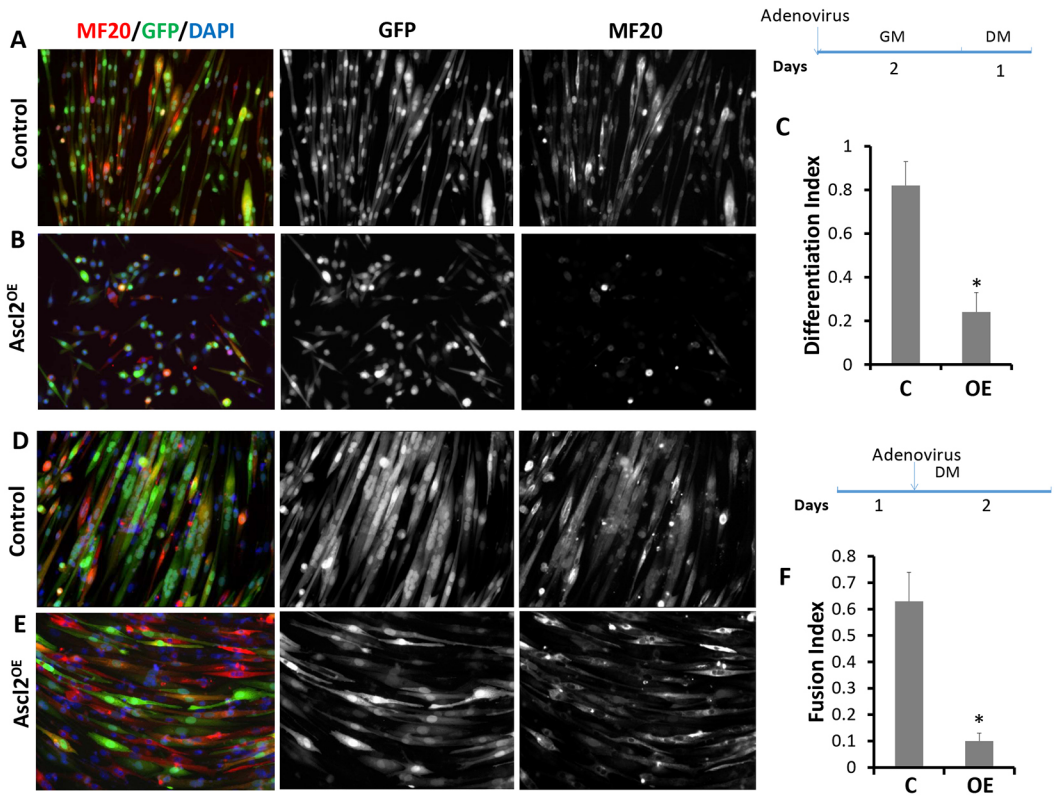

Fig. 4. Ascl2 inhibits the differentiation and fusion of myoblasts. (A,B) Control or Ascl2^{OE} myoblasts were induced to differentiate for 1 day. The differentiated myoblasts were stained by MF20 (red) and nuclei were counterstained with DAPI (blue). (C) Differentiation index of myoblasts. Only GFP^{+} cells were used for quantification. (D,E) Differentiated myoblasts were transduced with control or Ascl2^{OE} adenoviral vectors and then allowed to fuse for 2 more days. (F) Fusion index of myoblasts. *n*=3 different batches of primary myoblasts, with five different areas analyzed in each experiment. Error bars represent mean with s.d. of three independent biological replicates. *P<0.05 (Student's *t*-test). GM, growth media; DM, differentiation media.

muscle regeneration upon injury (Fig. S3B-D). Specifically, 73% of the cross-sectional areas were regenerated in the control muscles, whereas Ascl2^{OE} adenovirus-infected TA muscles had only 36% regenerated areas (Fig. S3B,C). In addition we labeled MyoD, an early marker of satellite cell activation, to determine the presence of activated myogenic cells. MyoD was not detectable in any Ascl2^{+} cells (Fig. S3E), resulting in fewer overall MyoD^{+} cells in Ascl2^{OE} muscles than in control muscles (Fig. S3F). Further, we colabeled MyoD and Pax7 to determine the percentage of Pax7^{+} MyoD^{-} and Pax7^{+} MyoD^{+} cells. Around 72% of Pax7^{+} cells were MyoD^{-} in control muscles (Fig. S3G,J). By contrast, 92% of Pax7^{+} cells were MyoD^{-} in Ascl2^{OE} muscles (Fig. S3H,J), indicating that Ascl2^{OE} inhibited the activation of satellite cells. Owing to the lack of activation and subsequent satellite cell proliferation, Ascl2^{OE} TA muscles contained fewer Pax7^{+} cells overall than control muscles (Fig. S3I). That Ascl2 inhibits satellite cell proliferation is also supported by the observation that none of the Ascl2^{+} cells was Ki67^{+} (Fig. S3K). qPCR analysis further confirmed decreased *Pax7*, *MyoD* (*Myod1*) and *Myog* levels in Ascl2^{OE} compared with control TA muscles (Fig. S3L).

At 14 dpi, Ascl2^{OE} muscles were 30% lighter than control muscles (Fig. 5C). Morphologically, the control TA muscles were fully replaced by newly regenerated myofibers characterized by centrally localized myonuclei (Fig. 5D). By contrast, Ascl2^{OE} muscles were only partially regenerated (Fig. 5E). Quantitatively, the control TA muscles had nearly 100% regenerated areas, whereas Ascl2^{OE} TA muscles only had ∼70% regenerated areas (Fig. 5F). In addition, we labeled MyoD and Pax7 in control and Ascl2^{OE} muscle sections (Fig. 5H). Although Ascl2^{OE} TA muscles had more MyoD^{+} cells at 14 dpi than at 7 dpi (Fig. S3F), they still contained fewer MyoD^{+} cells than control muscles at the same time (Fig. 5K). Consistently, mRNA levels of *MyoD* and *Myog* were lower in Ascl2^{OE} than in control TA muscles (Fig. 5G). However, Ascl2^{OE} TA muscles contained comparable numbers of Pax7^{+} cells as control muscles (Fig. 5J). Importantly, the percentage of Pax7^{+} MyoD^{-} satellite cells was still higher in Ascl2^{OE} muscles than in control muscles (Fig. 5I), indicating a role of Ascl2 in maintaining the quiescence of satellite cells.

At 30 dpi, the muscle structure was totally restored in control muscles (Fig. 5L). In Ascl2^{OE} muscles, however, the regenerated myofibers were very small (Fig. 5L) and the average weight of Ascl2^{OE} muscles was 40% lighter than that of control muscles (Fig. 5M). Notably, ∼28% of Ascl2^{OE} myofibers had diameters below 20 µm (Fig. 5N), as compared with only 3% of control myofibers (Fig. 5N). Accordingly, the percentages of myofibers with diameters above 20 µm were lower in Ascl2^{OE} than in control muscles (Fig. 5N). These results demonstrate that Ascl2 impairs muscle regeneration by inhibiting myogenesis.

Ascl2 forms complexes with E-proteins

We next investigated how Ascl2 inhibits myogenesis. MyoD and Myog are key factors orchestrating myogenesis, and their expression in TA muscles is inhibited by Ascl2^{OE} (Fig. 5G). We examined how Ascl2^{OE} affects MyoD and Myog expression in myoblasts. Primary myoblasts were transduced with *Ascl2* or *GFP* (control) adenovirus for 2 days. Interestingly, the mRNA and protein levels of MyoD were not affected by Ascl2^{OE} (Fig. 6A,B). However, Ascl2^{OE} led to a 27% reduction in *Myog* mRNA (Fig. 6A) and repressed the expression of

Development (2017) 144, 235-247 doi:10.1242/dev.138099

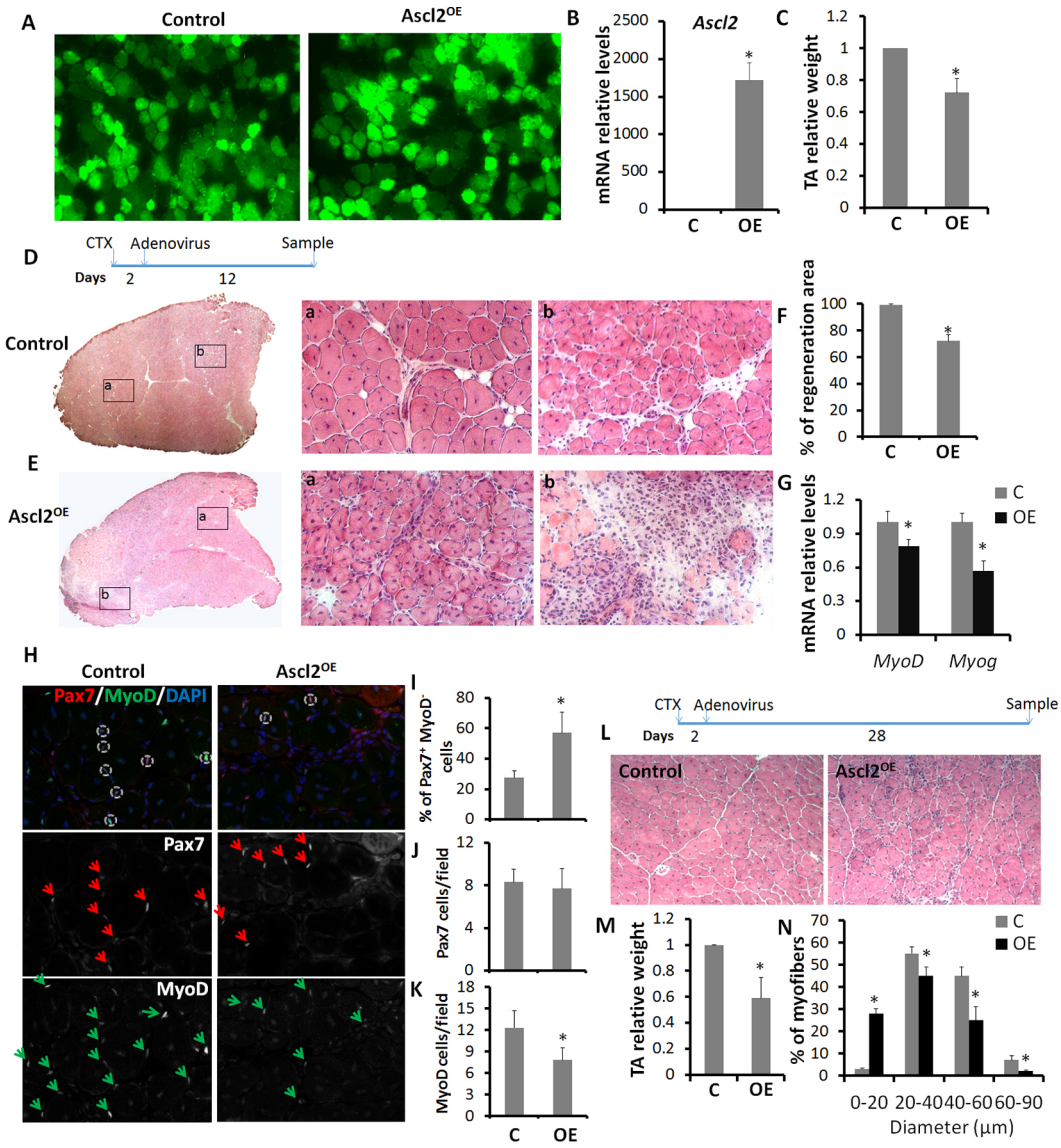

Fig. 5. Overexpression of Ascl2 impairs muscle regeneration. (A) GFP signals in TA muscles injected with adenovirus expressing GFP or Ascl2-GFP at 7 dpi. (B) Relative *Ascl2* mRNA levels in control and Ascl2^{OE} TA muscles at 7 dpi. (C) Relative weight of control and Ascl2^{OE} TA muscles at 14 dpi. (D,E) H&E staining of control (D) and Ascl2^{OE} (E) TA muscles at 14 dpi. Representative regions (Da,b,Ea,b) are shown at higher magnification. (F) Percentage of regeneration area of control and Ascl2^{OE} TA muscles at 14 dpi. (G) *MyoD* and *Myog* levels in control and Ascl2^{OE} TA muscles at 14 dpi. (H) Immunostaining of Pax7 (red, arrows), MyoD (green, arrows) and DAPI staining (blue) in control and Ascl2^{OE} TA muscles at 14 dpi. Circles indicate Pax^{+} MyoD^{+} cells. Five different areas were analyzed for each section, and four sections were analyzed for each sample. (I-K) The percentage of MyoD^{-} cells among Pax7^{+} cells (I), the number of Pax7^{+} cells per field (J) and the number of MyoD^{+} cells per field (K). (L) H&E staining of regenerated TA muscles at 30 dpi. (M) Relative weight of control and Ascl2^{OE} TA muscles at 30 dpi. (N) Myofiber size distribution in control and Ascl2^{OE} TA muscles at 30 dpi. Error bars represent mean with s.d. of four independent biological replicates. *P<0.05 (Student's t-test).

Myog at the protein level (Fig. 6B). In addition, expression of the proliferation-related factors *miR-133* (*Mir133*) and *Id3* was repressed by Ascl2^{OE} (Fig. S4A).

We next sought to determine how Ascl2^{OE} inhibits Myog expression. bHLH factors can block myogenesis through competitive binding with transcriptional coactivators (E-proteins) for E-boxes, or by forming inactive heterodimers with MRFs (Hsiao et al., 2009; Lemercier et al., 1998; Lu et al., 1999). To dissect how Ascl2 functions, we first sought to identify Ascl2-associated proteins. We used FLAG antibody to immunoprecipitate (IP) protein complexes from primary myoblasts transduced with *Ascl2-FLAG* or *GFP-FLAG* adenoviral vectors. Using mass spectrometry, we identified several E-proteins (TCF4, TCF12 and TCF3) specifically in Ascl2-associated complexes, but not in GFP-associated complexes (Table 1). IP analysis verified that TCF3 exists in an Ascl2-associated complex but not in a GFP-associated complex (Fig. 6C). These results suggest that Ascl2 interacts with classical E-proteins.

Ascl2 binds with E-proteins and E-boxes to repress the transcriptional activity of MRFs

As E-proteins function to activate the transcriptional activity of MyoD and Myog, we hypothesized that Ascl2 sequesters E-proteins to inhibit MyoD and Myog transcriptional activity. We used the E-box-dependent reporter 4R-tk-luc, which contains four tandem E-boxes from the *MCK* (*Ckm*) enhancer upstream of the thymidine kinase basal promoter (Weintraub et al., 1990), to test the

Development (2017) 144, 235-247 doi:10.1242/dev.138099

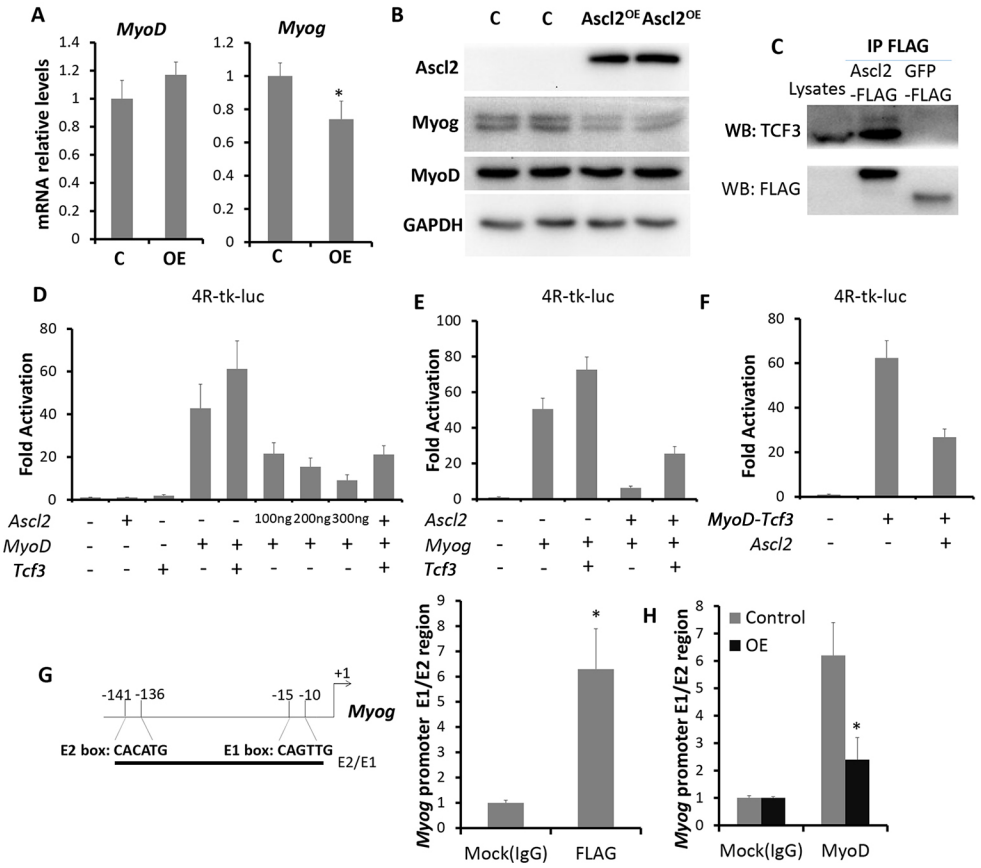

Fig. 6. Ascl2 inhibits the transcriptional activity of MRFs by competitive binding with E-proteins for E-boxes. (A,B) Relative expression of Myog and MyoD in control and Ascl2^{OE} myoblasts, as determined by qPCR (A) and western blot (B). (C) Detection of TCF3 in Ascl2-FLAG protein complexes but not in GFP-FLAG protein complexes. Myoblast lysate provided a positive control to indicate the position of TCF3. (D-F) Luciferase assays with 4R-tk-luc as the reporter. (G,H) Fold enrichments of the E-box region of the *Myog* promoter by Ascl2-FLAG (G) and MyoD (H), as determined by ChIP using antibodies against FLAG and MyoD, respectively. In each case, error bars represent the mean with s.d. of three independent biological replicates. **P*<0.05 (Student's *t*-test).

transcriptional activity of MyoD and Myog. Whereas Ascl2 or TCF3 alone was unable to activate the reporter (Fig. 6D), TCF3 enhanced, whereas Ascl2 inhibited, MyoD-dependent activation of the reporter in a dose-dependent manner (Fig. 6D). Similarly, TCF3 enhanced, but Ascl2 abolished, the transcriptional activity of Myog on the 4R-tk-luc reporter (Fig. 6E). Furthermore, Ascl2 inhibited the transcriptional activity of Myf6 on the 4R-tk-luc reporter (Fig. S4B). Importantly, inhibition of MyoD or Myog transcriptional activity by Ascl2 was rescued by addition of ectopic TCF3 (Fig. 6E,F), indicating that Ascl2 sequesters TCF3 to repress the transcriptional activity of MyoD, Myog and Myf6. To confirm this possibility, we performed luciferase assays using a tethered MyoD-TCF3 heterodimer that is resistant to sequestration (Berry et al., 1993). Whereas Ascl2 inhibited the transcriptional activity of MyoD by 80% (Fig. 6D), it only reduced the activity of MyoD-TCF3 by half (Fig. 6F). These results provide compelling biochemical evidence that Ascl2 represses the transcriptional activity of MRFs by sequestering E-proteins.

Table 1. Ascl2-associated proteins

Protein	Number of unique peptides identified	Total number of peptides	Sequence coverage (%)
Ascl2	12	12	44
TCF12 (HEB)	10	14	26
TCF4 (E2-2)	3	10	22
TCF3 (E2A)	2	5	9

Ascl2-associated proteins were identified by mass spectrometry from FLAG affinity-purified Ascl2 complexes.

The observation that Ascl2 only partially repressed the transcriptional activity of the tethered MyoD-TCF3 heterodimer suggests that Ascl2 might employ additional mechanism to repress the transcriptional activity of MRFs. As Ascl2 has been reported to bind E-box DNA motifs (Liu et al., 2014), we used chromatin immunoprecipitation (ChIP) to determine if Ascl2 directly binds to the two E-boxes in the proximal promoter of *Myog* (Fig. 6G). We transduced adenoviral *Ascl2-FLAG* vectors into primary myoblasts and used a FLAG antibody for ChIP analysis. As expected, a ChIP assay using FLAG antibody showed a 6-fold enrichment of E-box-containing DNA sequences compared with the control group using IgG antibody (Fig. 6G). As MyoD also binds to the E-boxes of the *Myog* promoter, we further investigated whether Ascl2 competes with MyoD for binding using Ascl2^{OE} myoblasts. ChIP assay using MyoD antibody showed that MyoD occupancy at the E-boxes of the *Myog* proximal promoter was significantly decreased in Ascl2^{OE} myoblasts (Fig. 6H). These results demonstrate that competitive binding for E-boxes is a secondary mechanism employed by Ascl2 to inhibit the transcriptional activity of MRFs.

The basic region of Ascl2 mediates its repressor function

Ascl2 and MRFs are classified as bHLH factors, but Ascl2 inhibits myogenesis whereas MRFs promote myogenesis. To understand the molecular mechanisms underlying these functional differences, we constructed chimeric proteins between Ascl2 and MyoD. First, the bHLH domain of Ascl2 was replaced by the MyoD bHLH domain, referred to as Ascl2(MyoD bHLH). Strikingly, whereas Ascl2 was unable to activate the 4R-tk-luc reporter, the Ascl2(MyoD bHLH) chimeric protein activated the reporter to the same level as MyoD (Fig. 7A). In addition, although Ascl2 reduces the transcriptional activity of MyoD (Fig. 6D), Ascl2(MyoD bHLH) marginally

Development (2017) 144, 235-247 doi:10.1242/dev.138099

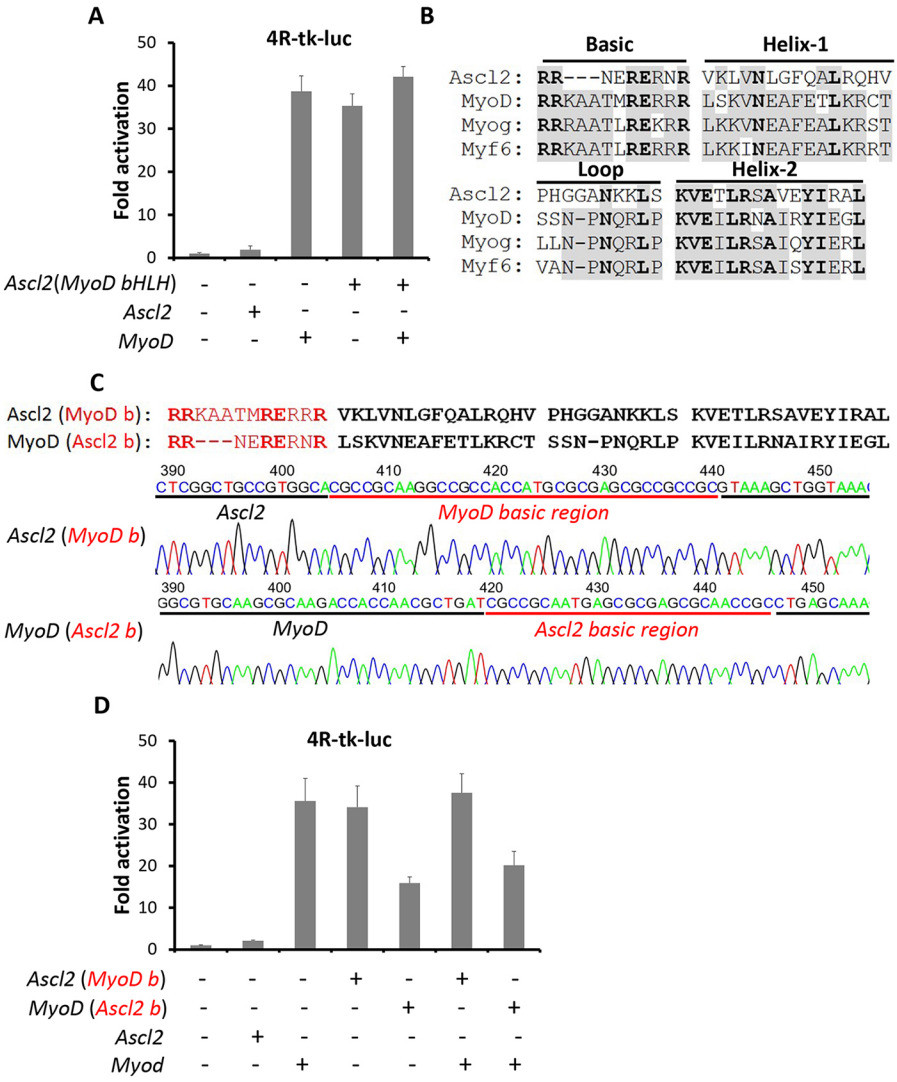

Fig. 7. The basic region determines Ascl2 function as an MRF inhibitor. (A,D) Luciferase assays with 4R-tk-luc as the reporter. Error bars represent the mean with s.d. of three independent biological replicates. (B) Amino acid alignment analysis of the bHLH domain of Ascl2 and three MRFs. Subdomains are indicated. (C) Schematic and sequencing results of the Ascl2 and MyoD chimeric bHLH domains.

enhanced the transcriptional activity of MyoD (Fig. 7A). These data indicate that the bHLH domain of Ascl2 is crucial for repressing MRFs.

To further define the subdomain within the Ascl2 bHLH domain that is required for transcriptional repression, we performed sequence alignment analysis of bHLH domains of Ascl2 and MRFs (Fig. 7B). The helix 1 and helix 2 domains are responsible for binding between bHLH factors (Davis et al., 1990). Despite the low conservation of helix 1 (33%) and helix 2 (66%) between Ascl2 and MRFs (Fig. 7B), the binding ability of Ascl2 to other bHLH factors, such as E-proteins, was not compromised (Table 1). We next compared the basic regions, which are responsible for DNA binding and myogenic activation (Brennan et al., 1991; Davis et al., 1990). Notably, the basic region of Ascl2 lacks three amino acids (KAA) that are common to MRFs (Fig. 7B). We therefore swapped the basic regions between Ascl2 and MyoD (Fig. 7C). Intriguingly, the Ascl2(MyoD b) construct activated the 4R-tk-luc reporter to the same level as MyoD (Fig. 7D). By contrast, the activity of MyoD (Ascl2 b) was decreased by 50%, as compared with that of MyoD (Fig. 7D). Furthermore, MyoD(Ascl2 b), but not Ascl2(MyoD b), inhibited the transcriptional activity of MyoD (Fig. 7D). These results indicate that the basic region determines the transcriptional repressor function of Ascl2.

MyoD and Myog rescue Ascl2^{OE}-induced myogenic blockage

To verify that Ascl2 inhibits myogenesis through repressing MRFs, we overexpressed MyoD or Myog in Ascl2^{OE} myoblasts. To achieve this, we co-transduced primary myoblasts with Ascl2^{OE} and MyoD^{OE} (or Myog^{OE} or control) adenoviral vectors. This approach led to 90% infection of myoblasts based on GFP signal (Fig. 8A). Similar to the results shown in Fig. 4A, Ascl2^{OE} myoblasts showed an obvious myogenic defect as indicated by the weak MF20 signals compared with the control group (Fig. 8A). Importantly, co-expression of MyoD (A+D) or Myog (A+G) efficiently rescued MF20 intensity to a level comparable to the control group (Fig. 8A). We further quantified the differentiation index and found that whereas 70% of nuclei were located in MF20^{+} cells in the control and rescue groups, only 16% cells were in MF20^{+} cells in the Ascl2^{OE} group (Fig. 8B).

At the gene expression level, *MyoD* and *Myog* mRNA levels were increased by 2.1-fold and 1.5-fold in the MyoD rescue group, and *Myog* mRNA levels were increased by 2.7-fold in the Myog rescue group (Fig. 8C). The mRNA levels of *eMHC* (*Myh3*), an indicator of myogenic differentiation, were indistinguishable among the two rescue groups and the control group (Fig. 8C). By contrast, the Ascl2^{OE} group had a 28% reduction in the mRNA levels of *Myog* and a 67% reduction of *eMHC* when compared with the control

Development (2017) 144, 235-247 doi:10.1242/dev.138099

group (Fig. 8C). These results demonstrate that MyoD and Myog rescue the myogenic defect of Ascl2^{OE} myoblasts and prove that Ascl2 inhibits myogenesis through repressing MRFs.

Ascl2 is activated by Notch1 signaling

To identify the upstream regulator of Ascl2 we focused on Notch signaling, which has been shown to activate *Ascl2* in epidermal cells in mice (Moriyama et al., 2008). We established *Pax7^{CreER}/ROSA-N1ICD* (Pax7-N1ICD^{OE}) mice that express a constitutively activated form of Notch1 (N1ICD) in satellite cells upon tamoxifen induction (Wen et al., 2012). Two-month-old male mice were treated with tamoxifen for 5 days followed by a 5-day chasing period to allow for Cre-mediated activation of N1ICD expression. Tamoxifen treatment of the Pax7-N1ICD^{OE} mice led to a 12-fold increase in *Heyl*, a direct target of N1ICD in TA muscles, accompanied by a 2-fold increase in *Ascl2* expression (Fig. 9A). In addition, we compared the *Ascl2* levels in control and Pax7-N1ICD^{OE} myoblasts after transducing *ROSA-N1ICD* myoblasts with *GFP* (control) or Cre adenoviral vectors. Compared with the control, the Cre vector transduction resulted in a 29-fold increase in *Heyl* and a 2-fold increase in *Ascl2* (Fig. 9B). However, the 2-fold increase in mRNA levels did not lead to detectable levels of Ascl2 protein in Pax7^{+} cells in cross-sections of TA muscles from adult Pax7-N1ICD^{OE} mice or Pax7-N1ICD^{OE} myoblasts (data not shown). These results indicate that Notch1 activation upregulates *Ascl2* transcription.

DISCUSSION

Ascl2 has been reported to play a role in placenta development, intestinal stem cell maintenance and follicular T-helper cell development (Guillemot et al., 1994; Liu et al., 2014; van der Flier et al., 2009), but its role in muscle tissues has not been reported. Our study has uncovered a novel role of Ascl2 in muscle stem cells. Ascl2 is expressed in a small subset of embryonic myoblasts that express Pax7 and MyoD at E12.5. These cells subsequently lose MyoD expression and become Pax7^{+} MyoD^{-} cells that form quiescent satellite cells during late fetal myogenesis (at E17.5). These results uncover a role of Ascl2 in the generation of satellite cells from embryonic myoblasts. The lack of Ascl2 expression in satellite cells of adult muscles indicates that Ascl2 is not required for the maintenance of satellite cells.

Embryonic myoblasts originate from Pax3^{+} cells (Messina and Cossu, 2009). We knocked out *Ascl2* in Pax3 lineage cells to investigate the role of Ascl2 in embryonic myoblasts. Loss of Ascl2 increased the expression of MyoD in Pax7^{+} cells, leading to an increased percentage of Pax7^{+} MyoD^{+} cells. As MyoD is able to induce myogenic differentiation (Rawls et al., 1998) and reduces myogenic progenitor cells (Vasyutina et al., 2007), MyoD

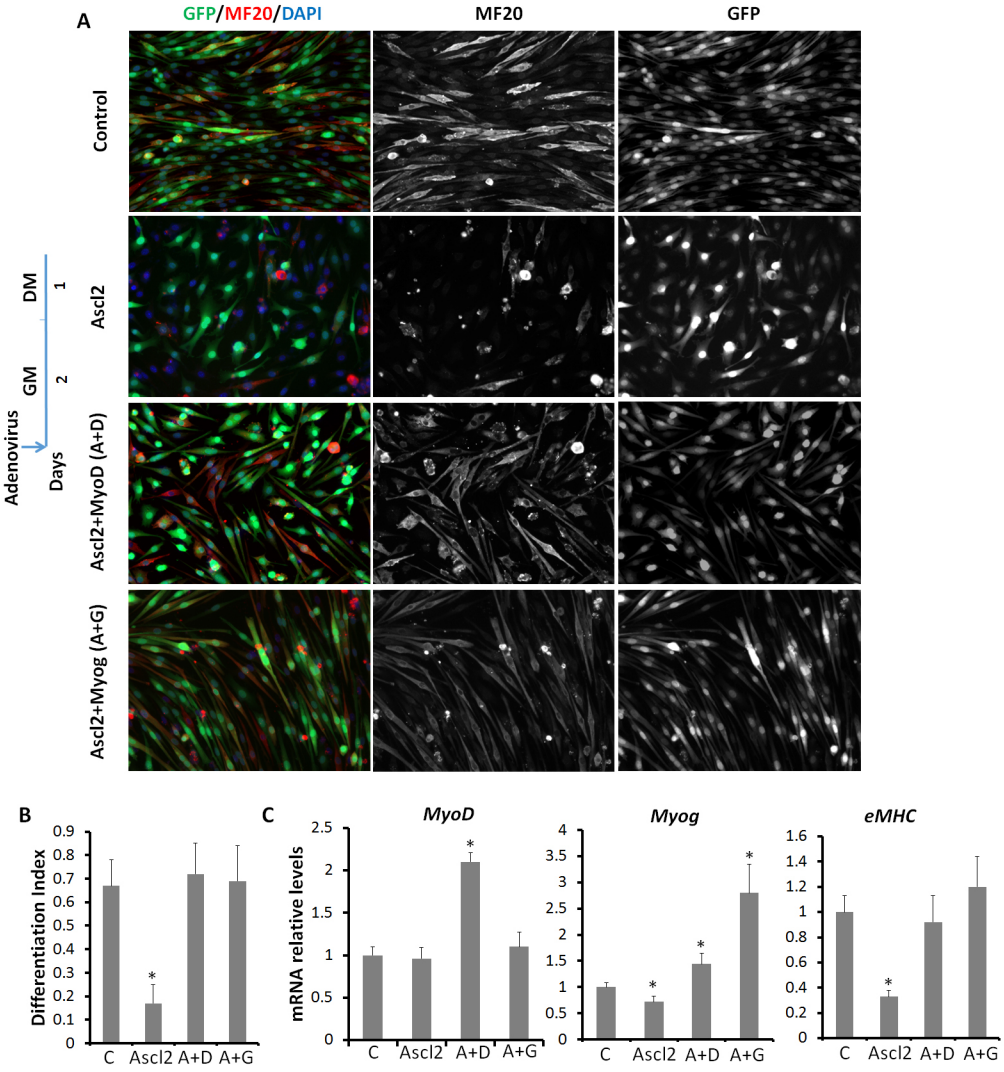

Fig. 8. MyoD and Myog rescue Ascl2^{OE}-induced myogenic blockage. (A) Control, Ascl2^{OE}, Ascl2^{OE}+MyoD^{OE} (A+D) and Ascl2^{OE}+Myog^{OE} (A+G) myoblasts were induced to differentiate for 1 day. The differentiated myoblasts were stained by MF20 (red) and nuclei were counterstained with DAPI (blue). Before induction of differentiation by serum withdrawal, myoblasts were incubated with adenoviruses for 1 day, and cultured in virus-free growth medium for 1 day more. (B) Differentiation index of myoblasts, calculated by dividing the number of nuclei in myotubes (MF20^{+} elongated cells) by the total number of nuclei. Only GFP^{+} cells were used for quantification. *n*=3 different batches of primary myoblasts, with five different areas analyzed in each experiment. (C) Relative expression of *MyoD*, *Myog* and *eMHC*. Error bars represent mean with s.d. of three independent biological experiments. **P*<0.05 (Student's *t*-test).

Development (2017) 144, 235-247 doi:10.1242/dev.138099

upregulation due to Ascl2 knockout leads to decreased myofiber size and body weight. As Pax3 is also expressed in Schwann cell precursors (Kioussi et al., 1995), we could not exclude the possibility that the decrease in body weight was also a result of the deletion of *Ascl2* in Schwann cells (Kury et al., 2002). The loss-of-function study indicates that Ascl2 facilitates the generation of $Pax7^+$ cells through repressing MyoD.

Next, we utilized the gain-of-function approach to study the function of Ascl2. Our *in vitro* results indicate that Ascl2 inhibits myoblast proliferation. To further investigate the *in vivo* role of Ascl2 in satellite cells and myoblasts, we used adenovirus to deliver *Ascl2* to TA muscles following CTX injection. In the CTX injury model, satellite cells are activated to participate in muscle regeneration. The high delivery efficiency indicated by the uniform GFP signal throughout the muscle sections and high *Ascl2* expression levels validated the efficacy of our *in vivo* model. In this *in vivo* model, $Ascl2^{OE}$ cells did not express MyoD, indicating that Ascl2 inhibited the expression of MyoD. As MyoD expression marks the activation of satellite cells and the subsequent proliferation of myoblasts (Zammit et al., 2004), this observation suggests that Ascl2 inhibits satellite cell activation and myoblast proliferation. Consistently, $Ascl2^{OE}$ cells did not express Ki67, a marker of proliferation. At the molecular level, MyoD activates the expression of *miR-133* and *Id3* to increase the proliferation of undifferentiated myoblasts (Chen et al., 2006; Rao et al., 2006; Wyzykowski et al., 2002). The decreased expression of *miR-133* and *Id3* in $Ascl2^{OE}$ cells can be explained by the decreased MyoD activity.

Ascl2 also repressed myoblast differentiation and fusion *in vitro*. In addition, the lower regenerative efficiency and smaller myofiber size of $Ascl2^{OE}$ muscles suggest that Ascl2 inhibits the differentiation and fusion of myoblasts *in vivo*. Interestingly, the expression of *MyoD* was not affected by Ascl2 at 2 dpi, but decreased at 7 dpi in $Ascl2^{OE}$ muscles. This can be explained by the reduced transcriptional activity of MyoD in $Ascl2^{OE}$ cells, which could lead to reduced MyoD expression, as MyoD activity could regulate its own expression (Tapscott, 2005). Through inhibiting MyoD activity and expression, Ascl2 indirectly increases the percentage of $Pax7^+$ $MyoD^-$ cells in $Ascl2^{OE}$ muscles. $Pax7^+$ $MyoD^+$ cells can, on the one hand, differentiate into $Pax7^-$ $MyoD^+$ $Myog^+$ myocytes; or, on the other hand, they can generate $Pax7^+$ $MyoD^-$ satellite cells through self-renewal (Motohashi and Asakura, 2014). Our finding that Ascl2 inhibits MRF activity and Myog expression suggests that Ascl2 blocks the differentiation of $Pax7^+$ $MyoD^+$ cells to $Pax7^-$ $MyoD^+$ $Myog^+$ myocytes. In turn, Ascl2 promotes $Pax7^+$ $MyoD^+$ cells to become quiescent $Pax7^+$ $MyoD^-$ cells (Fig. 9C). This function of Ascl2 is important for the generation of satellite cells from proliferating myoblasts because extensive differentiation induced by high MRF levels depletes the myogenic progenitor cells (Vasyutina et al., 2007).

Our mass spectrometry, biochemical and promoter assays demonstrate that Ascl2 represses MRF activity in at least two ways: through sequestering E-proteins and by competitively binding for E-boxes. We demonstrated that Ascl2 associated with E-proteins and verified that TCF3 could bind to Ascl2. In addition, TCF3 could partly relieve Ascl2 repression of the transcriptional activity of MRFs. As MRFs and transcriptional coactivators were not detected among the Ascl2 associated proteins, we excluded the possibility that Ascl2 inhibits myogenesis through competitive

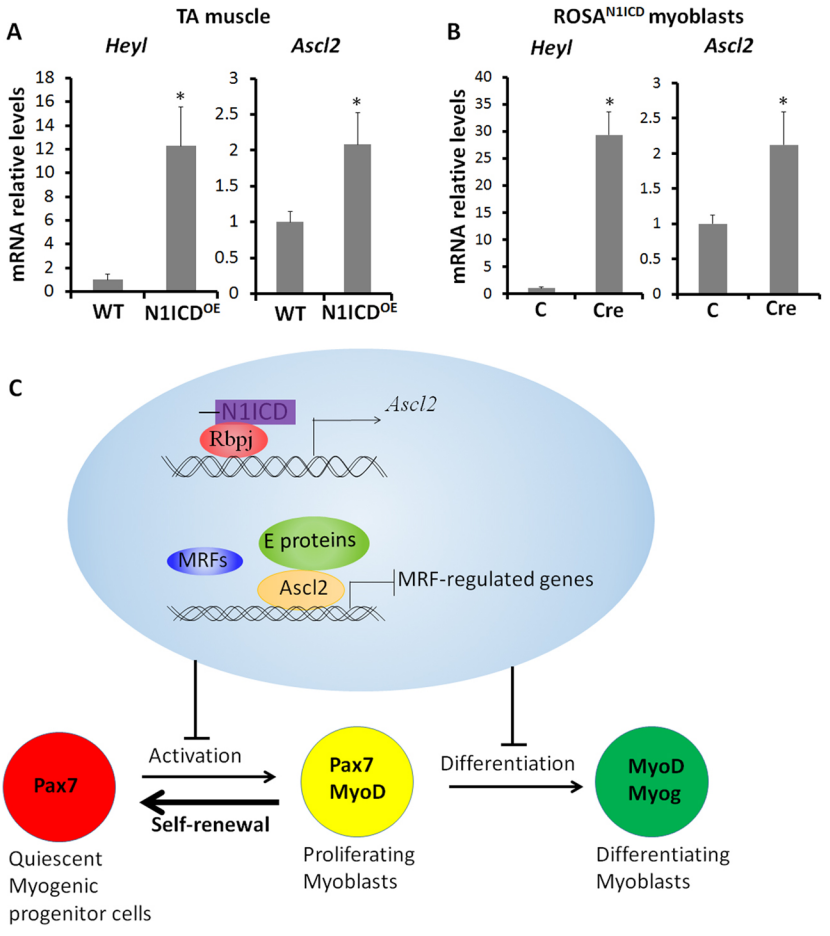

Fig. 9. N1ICD upregulates *Ascl2* in myoblasts. (A) Relative expression of *Heyl* and *Ascl2* in $Pax7^{CreER-}$/$N1ICD^{flox/+}$ (WT) and Pax7-N1ICD^{OE} TA muscles. Error bars represent mean with s.d. of four independent biological replicates. (B) Relative expression of *Heyl* and *Ascl2* in control and Pax7-N1ICD^{OE} myoblasts. Error bars represent mean with s.d. of three independent biological replicates. *P<0.05 (Student's t-test). (C) Model summarizing how Ascl2 modulates myogenesis. Activated myogenic progenitor cells ($Pax7^+$ $MyoD^+$) can either differentiate into $Pax7^-$ $MyoD^+$ $Myog^+$ myocytes or generate $Pax7^+$ $MyoD^-$ quiescent progenitor cells (satellite cells). Rbpj binds to the promoter of *Ascl2*, and the N1ICD-Rbpj complex directly activates *Ascl2*. Ascl2 represses MRFs by competitively binding with E-proteins to E-boxes, and inhibits the activation and differentiation of myoblasts, facilitating Notch signaling-induced myoblast self-renewal.

Development (2017) 144, 235-247 doi:10.1242/dev.138099

binding with transcriptional coactivators or by directly forming inactive heterodimers with MRFs. We verified that Ascl2 binds to E-boxes, consistent with a previous report (Liu et al., 2014). Additionally, we found that the binding of MyoD to the two E-boxes in the *Myog* promoter was significantly decreased in Ascl2^{OE} myoblasts, indicating that Ascl2 competes with MyoD for E-box binding.

Furthermore, we identified the basic region as the structural domain mediating Ascl2 transcriptional repressor function. The basic region is responsible for DNA binding and myogenic activation (Brennan et al., 1991; Davis et al., 1990). DNA binding and myogenic activation are two separate events (Brennan et al., 1991). Mutations in the basic regions have been reported to repress transcriptional activation without affecting DNA binding (Brennan et al., 1991). The amino acids following 'RR' in the basic region are indispensable for myogenic activation (Brennan et al., 1991; Davis et al., 1990). We found that the basic region of Ascl2 lacks three amino acids following 'RR'. This sequence structure suggests that Ascl2 binds to DNA but cannot activate myogenic gene expression, and explains how Ascl2 competes with MRFs for DNA binding sites and E-proteins. Importantly, the myogenic defect of Ascl2^{OE} myoblasts was rescued by overexpressing MyoD and Myog. These data prove that Ascl2 inhibits myogenesis through repressing the transcriptional activities of MRFs. Our study thus identifies Ascl2 as a novel member of the repressive bHLH factors [which include MyoR, Mist1 (Bhlha15) and Bhlhe40] that compete with MRFs for heterodimerization partners and E-boxes to modulate myogenesis (Hsiao et al., 2009; Lemercier et al., 1998; Lu et al., 1999; Wang et al., 2015).

We identified Notch signaling as a potential upstream regulator of *Ascl2*. The Notch signaling pathway is crucial for the self-renewal of satellite cells (Wen et al., 2012). We found that the constitutively active form of Notch1 (N1ICD) upregulated Ascl2 in both myoblasts and muscle tissues. Consistently, overexpression of N1ICD also upregulates *Ascl2* in adipose tissues (Bi et al., 2016). Our observation is consistent with the report that Rbpj binds to the promoter of *Ascl2*, and that the N1ICD-Rbpj complex directly activates *Ascl2* in skin epidermis (Moriyama et al., 2008). Therefore, Ascl2 possibly mediates the effect of Notch signaling in satellite cell self-renewal through repressing the transcriptional activity of MRFs (Fig. 9C). However, the 2-fold increase in *Ascl2* mRNA did not lead to detectable levels of Ascl2 protein, suggesting that other epigenetic mechanisms are involved in regulating Ascl2 expression in adult satellite cells. It would be interesting to identify these mechanisms in the future.

MATERIALS AND METHODS

Animals

Mice were obtained or derived as described in the supplementary Material and Methods. Mice were housed with free access to water and standard rodent chow. All procedures involving the use of animals were performed in accordance with the guidelines of Purdue University's Animal Care and Use Committee.

Primary myoblast isolation, culture and differentiation

Primary myoblasts were isolated from 5-week-old female mice as described (Wang et al., 2015). Detailed procedures are provided in the supplementary Materials and Methods.

Immunostaining and image acquisition

Antibody staining was performed as described (Wang et al., 2015). Further information, including details of the antibodies used, is provided in the supplementary Materials and Methods.

Western blot and real-time PCR

Protein expression and mRNA expression levels were assessed by western blot and real-time PCR, respectively, as described in the supplementary Materials and Methods and Table S1.

Adenovirus generation

The adenovirus with *Ascl2*, *MyoD* or *Myog* insertion was generated using the AdEasy system (Agilent). Detailed procedures are provided in the supplementary Materials and Methods.

Muscle injury and adenovirus injection

Muscle regeneration was induced by cardiotoxin (CTX; Sigma-Aldrich) injection. Mice were first anesthetized using a ketamine-xylazine cocktail and then the TA muscles were bilaterally injured with 50 µl 10 mM CTX. Two days after CTX injury, 50 µl concentrated adenovirus (1×10^{12} viral particles/ml) was injected into injured TA muscles. The left and right TA muscles were injected with Ascl2-expressing and control adenovirus, respectively. Muscles were harvested at 5, 12 and 28 days post injection of adenovirus.

Cryosectioning and H&E staining

Fresh samples were embedded in OCT compound (Sakura) and frozen in isopentane chilled on dry ice-ethanol slurry. Embedded samples were cut into 10-µm-thick cross-sections using a Leica CM1850 cryostat. Hematoxylin and Eosin (H&E)-stained images were captured with a Nikon D90 digital camera installed on a Nikon (Diaphot) inverted microscope.

Ascl2 binding complex extraction and mass spectrometry data acquisition

Plasmids containing *Ascl2-FLAG* or *GFP-FLAG* were transduced into primary myoblasts (70-80% confluence) by adenovirus. The Ascl2 binding complex was extracted using anti-FLAG magnetic bead slurry (Sigma, M8823). The complex was further analyzed with a high-resolution hybrid dual-cell linear ion trap LTQ-Orbitrap Velos mass spectrometer (Thermo Fisher). For details, see the supplementary Materials and Methods.

Construction of chimeric proteins between Ascl2 and MyoD

Chimeric proteins between Ascl2 and MyoD were constructed using modified overlap extension PCR (Li et al., 2016). Further information, including details of the primers used, is provided in the supplementary Materials and Methods and Table S1.

Luciferase assay

Transient transfections were performed with Lipofectamine 2000 (Thermo Scientific) according to the manufacturer's instructions. HEK293 cells were grown in Dulbecco's modified Eagle's medium (DMEM) supplemented with 10% FBS. Details of the plasmids used are provided in the supplementary Materials and Methods.

ChIP

The commercial Ascl2 antibody was not suitable for ChIP, so we transduced adenoviral Ascl2-FLAG plasmid into primary myoblasts in growth medium. The treated primary myoblasts were cross-linked with 1% formaldehyde in Ham's F-10 medium for 10 min at room temperature followed by the addition of 125 mM glycine for 5 min at room temperature, after which cells were scraped into SDS lysis buffer. The cells were further sonicated and diluted for immunoprecipitation with the indicated antibodies. Immunoprecipitates were eluted and cross-links reversed overnight at 65°C. DNA fragments were purified using the Cycle Pure Kit (Omega Bio-tek), and the myogenin promoter E1/E2 region quantified by real-time PCR. Further details are provided in the supplementary Materials and Methods.

Statistical analysis

Data are presented with mean±s.e.m. *P*-values were calculated using an unpaired two-tailed Student's *t*-test. $P<0.05$ was considered statistically significant.

Acknowledgements
We thank Dr Stephen Konieczny (Biological Sciences, Purdue University) for generously providing 4R-tk-luc, pcDNA3.1-*E47* and pECE-*MyoD-E47* plasmids; Dr Sarah Calve (Biomedical Engineering, Purdue University) for sharing animals (embryos); Jun Wu for mouse colony maintenance; and members of the S.K. laboratory for valuable comments.

Competing interests
The authors declare no competing or financial interests.

Author contributions
C.W. and S.K. conceived the project, designed the experiments and prepared the manuscript. C.W., M.W., F.Y., T.S. and Y.N. performed the experiments. J.A. and W.A.T. performed mass spectrometry and analyzed data.

Funding
This work was supported by a grant from the US National Institutes of Health (R01AR060652 to S.K.) and a Purdue incentive grant from Purdue University Office of Vice President for Research (OVPR) to S.K. Deposited in PMC for release after 12 months.

Supplementary information
Supplementary information available online at
http://dev.biologists.org/lookup/doi/10.1242/dev.138099.supplemental

References

Bentzinger, C. F., Wang, Y. X. and Rudnicki, M. A. (2012). Building muscle: molecular regulation of myogenesis. *Cold Spring Harb. Perspect. Biol.* **4**, pii: a008342.
Berry, M. J., Banu, L., Harney, J. W. and Larsen, P. R. (1993). Functional characterization of the eukaryotic secis elements which direct selenocysteine insertion at UGA codons. *EMBO J.* **12**, 3315-3322.
Bi, P., Yue, F., Karki, A., Castro, B., Wirbisky, S. E., Wang, C., Durkes, A., Elzey, B. D., Andrisani, O. M., Bidwell, C. A. et al. (2016). Notch activation drives adipocyte dedifferentiation and tumorigenic transformation in mice. *J. Exp. Med.* **213**, 2019-2037.
Braun, T., Buschhausendenker, G., Bober, E., Tannich, E. and Arnold, H. H. (1989). A novel human-muscle factor related to but distinct from Myod1 induces myogenic conversion in 10T1/2 fibroblasts. *EMBO J.* **8**, 701-709.
Brennan, T. J., Chakraborty, T. and Olson, E. N. (1991). Mutagenesis of the myogenin basic region identifies an ancient protein motif critical for activation of myogenesis. *Proc. Natl. Acad. Sci. USA* **88**, 5675-5679.
Chen, J.-F., Mandel, E. M., Thomson, J. M., Wu, Q., Callis, T. E., Hammond, S. M., Conlon, F. L. and Wang, D.-Z. (2006). The role of microRNA-1 and microRNA-133 in skeletal muscle proliferation and differentiation. *Nat. Genet.* **38**, 228-233.
Davis, R. L., Weintraub, H. and Lassar, A. B. (1987). Expression of a single transfected cdna converts fibroblasts to myoblasts. *Cell* **51**, 987-1000.
Davis, R. L., Cheng, P.-F., Lassar, A. B. and Weintraub, H. (1990). The MyoD DNA binding domain contains a recognition code for muscle-specific gene activation. *Cell* **60**, 733-746.
Edmondson, D. G. and Olson, E. N. (1989). A gene with homology to the myc similarity region of MyoD1 is expressed during myogenesis and is sufficient to activate the muscle differentiation program. *Genes Dev.* **3**, 628-640.
Günther, S., Kim, J., Kostin, S., Lepper, C., Fan, C.-M. and Braun, T. (2013). Myf5-positive satellite cells contribute to Pax7-dependent long-term maintenance of adult muscle stem cells. *Cell Stem Cell* **13**, 590-601.
Guillemot, F., Nagy, A., Auerbach, A., Rossant, J. and Joyner, A. L. (1994). Essential role of Mash-2 in extraembryonic development. *Nature* **371**, 333-336.
Hasty, P., Bradley, A., Morris, J. H., Edmondson, D. G., Venuti, J. M., Olson, E. N. and Klein, W. H. (1993). Muscle deficiency and neonatal death in mice with a targeted mutation in the myogenin gene. *Nature* **364**, 501-506.
Hsiao, S. P., Huang, K. M., Chang, H. Y. and Chen, S. L. (2009). P/CAF rescues the bhlhe40-mediated repression of myod transactivation. *Biochem. J.* **422**, 343-352.
Johnson, J. E., Birren, S. J. and Anderson, D. J. (1990). Two rat homologues of Drosophila achaete-scute specifically expressed in neuronal precursors. *Nature* **346**, 858-861.
Kanisicak, O., Mendez, J. J., Yamamoto, S., Yamamoto, M. and Goldhamer, D. J. (2009). Progenitors of skeletal muscle satellite cells express the muscle determination gene, myod. *Dev. Biol.* **332**, 131-141.
Kassar-Duchossoy, L., Gayraud-Morel, B., Gomès, D., Rocancourt, D., Buckingham, M., Shinin, V. and Tajbakhsh, S. (2004). Mrf4 determines skeletal muscle identity in Myf5: Myod double-mutant mice. *Nature* **431**, 466-471.
Kassar-Duchossoy, L., Giacone, E., Gayraud-Morel, B., Jory, A., Gomes, D. and Tajbakhsh, S. (2005). Pax3/pax7 mark a novel population of primitive myogenic cells during development. *Genes Dev.* **19**, 1426-1431.
Kioussi, C., Gross, M. K. and Gruss, P. (1995). Pax3: a paired domain gene as a regulator in PNS myelination. *Neuron* **15**, 553-562.
Kuang, S. and Rudnicki, M. A. (2008). The emerging biology of satellite cells and their therapeutic potential. *Trends Mol. Med.* **14**, 82-91.
Kuang, S., Kuroda, K., Le Grand, F. and Rudnicki, M. A. (2007). Asymmetric self-renewal and commitment of satellite stem cells in muscle. *Cell* **129**, 999-1010.
Kury, P., Greiner-Petter, R., Cornely, C., Jurgens, T. and Muller, H. W. (2002). Mammalian achaete scute homolog 2 is expressed in the adult sciatic nerve and regulates the expression of Krox24, Mob-1, Cxcr4, and p57kip2 in schwann cells. *J. Neurosci.* **22**, 7586-7595.
Lassar, A. B., Davis, R. L., Wright, W. E., Kadesch, T., Murre, C., Voronova, A., Baltimore, D. and Weintraub, H. (1991). Functional activity of myogenic HLH proteins requires hetero-oligomerization with E12/E47-like proteins in vivo. *Cell* **66**, 305-315.
Lemercier, C., To, R. Q., Carrasco, R. A. and Konieczny, S. F. (1998). The basic helix-loop-helix transcription factor Mist1 functions as a transcriptional repressor of myod. *EMBO J.* **17**, 1412-1422.
Li, Z., Wang, C., Jiang, F., Huan, P. and Liu, B. (2016). Characterization and expression of a novel caspase gene: Evidence of the expansion of caspases in *Crassostrea gigas*. *Comp. Biochem. Physiol. B Biochem. Mol. Biol.* **201**, 37-45.
Liu, X., Chen, X., Zhong, B., Wang, A., Wang, X., Chu, F., Nurieva, R. I., Yan, X., Chen, P., van der Flier, L. G. et al. (2014). Transcription factor achaete-scute homologue 2 initiates follicular t-helper-cell development. *Nature* **507**, 513.
Lu, J., Webb, R., Richardson, J. A. and Olson, E. N. (1999). MyoR: a muscle-restricted basic helix-loop-helix transcription factor that antagonizes the actions of myod. *Proc. Natl. Acad. Sci. USA* **96**, 552-557.
Mauro, A. (1961). Satellite cell of skeletal muscle fibers. *J. Biophys. Biochem. Cytol.* **9**, 493.
Messina, G. and Cossu, G. (2009). The origin of embryonic and fetal myoblasts: a role of Pax3 and Pax7. *Genes Dev.* **23**, 902-905.
Moriyama, M., Durham, A.-D., Moriyama, H., Hasegawa, K., Nishikawa, S.-I., Radtke, F. and Osawa, M. (2008). Multiple roles of notch signaling in the regulation of epidermal development. *Dev. Cell* **14**, 594-604.
Motohashi, N. and Asakura, A. (2014). Muscle satellite cell heterogeneity and self-renewal. *Frontiers Cell Dev. Biol.* **2**, 1.
Olson, E. N. and Klein, W. H. (1994). bHLH factors in muscle development: dead lines and commitments, what to leave in and what to leave out. *Genes Dev.* **8**, 1-8.
Pownall, M. E., Gustafsson, M. K. and Emerson, C. P. (2002). Myogenic regulatory factors and the specification of muscle progenitors in vertebrate embryos. *Annu. Rev. Cell. Dev. Biol.* **18**, 747-783.
Rao, P. K., Kumar, R. M., Farkhondeh, M., Baskerville, S. and Lodish, H. F. (2006). Myogenic factors that regulate expression of muscle-specific microRNAs. *Proc. Natl. Acad. Sci. USA* **103**, 8721-8726.
Rawls, A., Valdez, M. R., Zhang, W., Richardson, J., Klein, W. H. and Olson, E. N. (1998). Overlapping functions of the myogenic bhlh genes mrf4 and myod revealed in double mutant mice. *Development* **125**, 2349-2358.
Relaix, F., Rocancourt, D., Mansouri, A. and Buckingham, M. (2005). A pax3/pax7-dependent population of skeletal muscle progenitor cells. *Nature* **435**, 948-953.
Rhodes, S. J. and Konieczny, S. F. (1989). Identification of MRF4: a new member of the muscle regulatory factor gene family. *Genes Dev.* **3**, 2050-2061.
Rudnicki, M. A., Schnegelsberg, P. N. J., Stead, R. H., Braun, T., Arnold, H.-H. and Jaenisch, R. (1993). MyoD or Myf-5 is required for the formation of skeletal muscle. *Cell* **75**, 1351-1359.
Sambasivan, R., Comai, G., Le Roux, I., Gomès, D., Konge, J., Dumas, G., Cimper, C. and Tajbakhsh, S. (2013). Embryonic founders of adult muscle stem cells are primed by the determination gene mrf4. *Dev. Biol.* **381**, 241-255.
Tapscott, S. J. (2005). The circuitry of a master switch: Myod and the regulation of skeletal muscle gene transcription. *Development* **132**, 2685-2695.
van der Flier, L. G., van Gijn, M. E., Hatzis, P., Kujala, P., Haegebarth, A., Stange, D. E., Begthel, H., van den Born, M., Guryev, V., Oving, I. et al. (2009). Transcription factor achaete scute-like 2 controls intestinal stem cell fate. *Cell* **136**, 903-912.
Vasyutina, E., Lenhard, D. C., Wende, H., Erdmann, B., Epstein, J. A. and Birchmeier, C. (2007). Rbp-j (Rbpsuh) is essential to maintain muscle progenitor cells and to generate satellite cells. *Proc. Natl. Acad. Sci. USA* **104**, 4443-4448.
Wang, C., Liu, W., Liu, Z., Chen, L., Liu, X. and Kuang, S. (2015). Hypoxia inhibits myogenic differentiation through p53 protein-dependent induction of Bhlhe40 protein. *J. Biol. Chem.* **290**, 29707-29716.
Weintraub, H., Davis, R., Lockshon, D. and Lassar, A. (1990). MyoD binds cooperatively to two sites in a target enhancer sequence: occupancy of two sites is required for activation. *Proc. Natl. Acad. Sci. USA* **87**, 5623-5627.

Development (2017) 144, 235-247 doi:10.1242/dev.138099

Wen, Y., Bi, P., Liu, W., Asakura, A., Keller, C. and Kuang, S. (2012). Constitutive Notch activation upregulates pax7 and promotes the self-renewal of skeletal muscle satellite cells. *Mol. Cell. Biol.* **32**, 2300-2311.

Wyzykowski, J. C., Winata, T. I., Mitin, N., Taparowsky, E. J. and Konieczny, S. F. (2002). Identification of novel MyoD gene targets in proliferating myogenic stem cells. *Mol. Cell. Biol.* **22**, 6199-6208.

Zammit, P. S., Heslop, L., Hudon, V., Rosenblatt, J. D., Tajbakhsh, S., Buckingham, M. E., Beauchamp, J. R. and Partridge, T. A. (2002). Kinetics of myoblast proliferation show that resident satellite cells are competent to fully regenerate skeletal muscle fibers. *Exp. Cell Res.* **281**, 39-49.

Zammit, P. S., Golding, J. P., Nagata, Y., Hudon, V., Partridge, T. A. and Beauchamp, J. R. (2004). Muscle satellite cells adopt divergent fates: a mechanism for self-renewal? *J. Cell Biol.* **166**, 347-357.

Zhang, J.-M., Chen, L., Krause, M., Fire, A. and Paterson, B. M. (1999). Evolutionary conservation of myod function and differential utilization of E proteins. *Dev. Biol.* **208**, 465-472.